

Practical and Theoretical Aspects of Three-Dimensional Homonuclear Hartmann-Hahn-Nuclear Overhauser Enhancement Spectroscopy of Proteins

HARTMUT OSCHKINAT,* CHRISTIAN CIESLAR,* TADEUSZ A. HOLAK,*
G. MARIUS CLORE,*†‡ AND ANGELA M. GRONENBORN*†‡

*Max-Planck Institut für Biochemie, D-8033 Martinsried bei München, West Germany, and
†Laboratory of Chemical Physics, National Institute of Diabetes and Digestive and
Kidney Diseases, National Institutes of Health, Bethesda, Maryland 20892

Received October 28, 1988

The practical and theoretical aspects of three-dimensional homonuclear Hartmann-Hahn-nuclear Overhauser enhancement spectroscopy (3D HOHAHA-NOESY) are presented and illustrated using the protein α_1 -purothionin as an example. A number of sequences are proposed with frequency selection either in the F_1 dimension only or in both the F_1 and the F_2 dimensions, and their relative merits are discussed, particularly with respect to spectral resolution and measurement time. In addition, the nature of the various signals arising in 3D homonuclear spectroscopy, methods of evaluation of 3D HOHAHA-NOESY spectra, and the expected patterns of 3D cross peaks for different secondary structure elements in proteins are considered. © 1989 Academic Press, Inc.

Three-dimensional NMR (1-6) has been proposed as a method for extending the methodology of protein structure determination by NMR to larger molecular weight systems ($M_r > 10,000$) (7, 8). By extending 2D NMR spectra into a third dimension using another chemical-shift parameter, 3D NMR spectroscopy allows one to resolve overlapping or degenerate cross peaks present in 2D spectra. One application of 3D NMR spectroscopy is the dispersion of the homonuclear ^1H 2D NOESY (9) spectrum into a third dimension by the chemical shifts of the coupled spins. The latter may be protons (1-4) or heteronuclei such as ^{15}N or ^{13}C (5, 6). We have recently demonstrated the applicability of the homonuclear 3D HOHAHA-NOESY experiment (3, 4) which is a combination of the 2D homonuclear Hartmann-Hahn (9, 10) and 2D nuclear Overhauser enhancement (11) experiments, for the study of proteins. In this paper, we describe in detail the practical and theoretical aspects of this experiment.

To restrict both measurement time and amount of data collected, subvolumes of the full 3D spectrum may be recorded by selecting spectral ranges in F_1 and F_2 (1-4). This may not always be the best solution. We therefore discuss the relative merits of frequency selection in 3D spectroscopy. We show that recording the full spectral

‡ To whom correspondence should be addressed at the Laboratory for Chemical Physics, Building 2, Room 123, National Institute of Diabetes and Digestive and Kidney Diseases, National Institutes of Health, Bethesda, Maryland 20892.

width in F_2 and restricting the spectral width in F_1 only does not increase significantly the measurement time required to obtain a spectrum with comparable resolution to one with frequency selection in both F_1 and F_2 . In this context, two pulse sequences are described for recording 3D HOHAHA-NOESY with a reduced spectral width in F_1 .

The 3D cross peaks arise as a result of a twofold coherence transfer. Hence, in the context of homonuclear proton experiments, they are generally expected to be weak, especially for 3D spectra of proteins. We therefore discuss the sort of information that can be expected in a 3D HOHAHA-NOESY spectrum using the protein α_1 -purothionin as an example. This protein was chosen because its structure is known (12, 13) and it has a variety of secondary structure elements such as loops, α helices, and a β sheet. As in 2D NMR, certain distinct patterns arise in the 3D spectra as a result of particular through-space and through-bond coupling patterns associated with each of these different structural elements.

3D NMR SPECTROSCOPY, RESOLUTION, AND SELECTIVE EXCITATION

A 3D NMR spectrum describes the response of a spin system in 3D frequency space. The general experimental scheme for 3D NMR experiments is analogous to that for 2D NMR (14),

preparation— t_1 —mixing 1— t_2 —mixing 2—acquisition (t_3),

with a preparation pulse, two evolution periods t_1 and t_2 , two mixing periods, and an acquisition period t_3 . Three-dimensional Fourier transformation of the time-domain signal $s(t_1, t_2, t_3)$ yields the 3D spectrum $s(F_1, F_2, F_3)$. The key difference from 2D NMR is the additional evolution period t_2 which gives rise to the third dimension.

The implementation of 3D NMR spectroscopy was originally hampered by experimental and technical difficulties in achieving satisfactory resolution in all three dimensions. In particular, the data storage capacity of the computers commonly used in NMR spectrometers was too small to handle a full 3D spectrum and the tools to select frequency ranges within a ^1H NMR spectrum were not sufficiently developed to permit the easy recording of a subvolume of the full 3D spectrum. Both restrictions no longer pose insurmountable problems, as computers have become more powerful and relatively clean selection of frequency ranges can be obtained using semiselective shaped pulses such as Gaussian pulses (15, 16). The first 3D spectra were recorded using semiselective pulses in the preparation and mixing period (1-3) in a manner analogous to that proposed for some 2D experiments (17, 18). This approach, however, does not necessarily save experimental time, as the pulse sequences used to record a subvolume of the full 3D spectrum may need a longer minimum phase cycle. In this context we propose a homonuclear 3D experiment with frequency selection in the F_1 dimension only.

A major experimental problem in the general use of 3D spectroscopy is the *total experiment time* needed to record a spectrum with *adequate limiting resolution* (18). This is determined in practice by the stability of the NMR spectrometer. In contrast, the amount of data collected does not pose a real problem.

Due to the nature of the 3D pulse sequences, more extensive phase-cycling procedures are necessary than for the simple 2D techniques to select the desired coherence-

transfer pathways. Further, some 3D techniques require additional phase cycling for the suppression of artifacts. At the same time, the number of experiments that must be recorded to improve resolution increases with the power 2. The smallest possible phase cycle for a 3D experiment is four. This involves selection of the coherences $\Delta p = \pm 0, 2, 4, \dots$ for both mixing processes, as in the case of COSY–COSY, HOHAHA–ROESY, and HOHAHA–HOHAHA experiments. If one were to record a 3D spectrum with a spectral width of 14 ppm (appropriate for a protein) consisting of 512 data points in F_1 and F_2 , respectively, with a duration of 1.2 s per transient, corresponding to typical parameters of a routine 2D spectrum, the total experiment time would be 14 days, and the limiting resolution would be 16.5 Hz in both dimensions which is quite adequate for proteins at 500 MHz. The characterization of cross peaks by three frequencies in 3D NMR makes it easier to evaluate spectra of lower resolution than in 2D NMR, so that one may opt to record spectra with only 256 experiments in t_1 and t_2 . This would take 87 h, which is an acceptable measurement time. As in 2D spectroscopy, F_3 can be the axis with the best possible resolution, thereby permitting the resolution to be relaxed in one of the other two dimensions.

An additional problem must be dealt with when recording spectra of protein samples in 90% H₂O, as all approaches for the efficient suppression of the intense water resonance require further phase cycling. In some cases, it may be possible to use incoherent presaturation without phase cycling of the decoupler phases, thereby keeping a phase cycle of four. In practice, however, we have found that this procedure generates large amounts of noise. A further drawback of preirradiation is that it is also necessary to irradiate during the entire mixing time in order to avoid recovery of the water resonance. In the case of the 3D HOHAHA–NOESY experiment, efficient water suppression can be achieved using a jump–return read pulse (19) at the end of the sequence. The minimum phase cycle for this technique is eight, assuming that a very limited phase cycling for the NOESY unit is chosen. To record a full spectrum with 256 experiments in both dimensions would then require 7.3 days, which is probably too long for most practical applications. If only 200 experiments are taken in both dimensions, the total experiment time is 4.4 days which, although long, is acceptable. If, however, one records an experiment of this type using frequency selection in both the F_1 and the F_2 dimensions, one would need a much longer phase cycle so that the measurement time would not decrease substantially. On the other hand, frequency selection in only one dimension—preferably F_1 —would result in a considerable decrease in measurement time, as a spectrum with 64 experiments in t_1 and 256 experiments in t_2 would last only 43 h for a phase cycle of eight. In addition, the option of obtaining spectra with higher resolution exists.

Figure 1 depicts schematically the subvolumes resulting from different types of frequency selection. The full 3D spectrum is sketched for a spectral range of 14 ppm, typical of the complete chemical-shift range of a protein. The region recorded with frequency selection in F_1 only is that between 1.6 and 5.6 ppm in F_1 in the upper half of the cube; the region obtained by double frequency selection is shown in the lower half. These two subvolumes cover a substantial region of the entire 3D spectrum.

SIGNALS IN 3D NMR SPECTRA

There is a clear analogy between 3D NMR spectroscopy and 2D relayed experiments (20, 21), which arises from the two coherence-transfer steps in the pulse se-

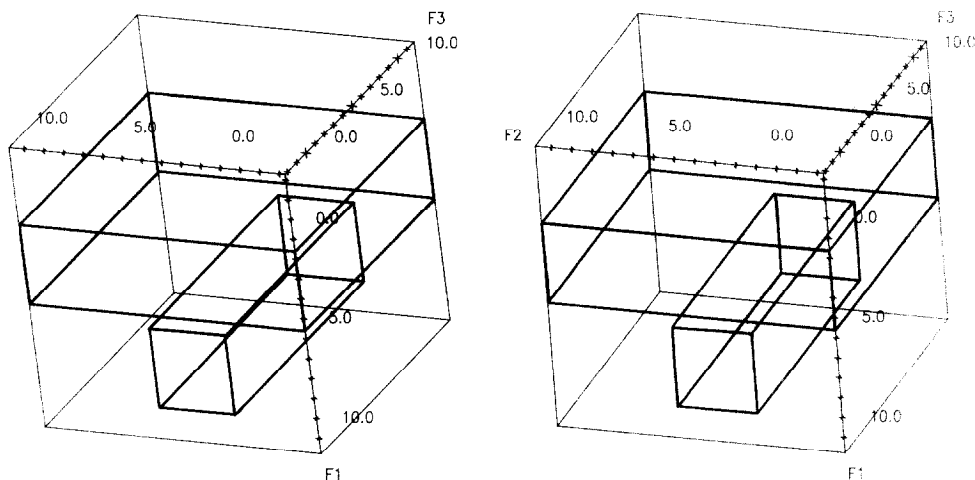


FIG. 1. Schematic representation of the subvolumes of a ^1H 3D HOHAHA-NOESY spectrum. Depending on the manner of frequency selection, either a slice of the cube along F_1 (indicated in the upper half of the spectrum) or a subcube with a reduced spectral width in F_1 and F_2 (indicated in the lower half of the spectrum) may be recorded.

quences before the detection of the signal. In homonuclear 2D techniques which correlate only single-quantum coherences (as opposed to 2D multiple-quantum spectroscopy and J, δ -resolved spectroscopy) there are axial peaks, cross peaks, and diagonal peaks, of which the axial peaks are removed by phase cycling. In 2D relayed spectroscopy, each of the latter two are composed of different contributions which can be characterized by their different "magnetization transfer pathways" (22).

The diagonal peaks in a 2D relayed spectrum consist of the superposition of two processes. The major contribution results from coherences which do not take part in any coherence transfer (the spins between which the transfer occurs are named A, B, C; the spins whose frequencies are observed in the spectrum are indicated with bold letters):



Additionally, there are contributions to the diagonal which result from a transfer to another spin and back to the primary excited spin:



For macromolecules, these cross peaks can be large especially in experiments that employ a NOE-dependent coherence transfer in one of the steps, as two protons which exhibit a scalar coupling via three bonds will always be close in space ($<4 \text{ \AA}$).

The cross peaks in a 2D relayed spectrum may arise either through a single magnetization transfer



or through a double magnetization transfer



In spectra of complicated spin systems, a single cross peak in a 2D relayed spectrum may be composed of several contributions. It is one of the advantages of 3D NMR spectroscopy that the overlap of contributions due to different pathways in one cross peak no longer occurs, as they will be separated in the third dimension by the frequency of the intermediate spin. Because of this feature, the signals in 3D NMR spectra are purely absorptive, rendering the 3D NMR experiment superior to 2D relayed spectroscopy.

Considering the full homonuclear 3D NMR spectrum as a cube, the different classes of signals discussed above will appear in different regions within the cube (Fig. 2). The signals with three identical frequencies arising from the "nonprocess" $A \rightarrow A \rightarrow A$ occur on a diagonal through the cube from the edge with the coordinates $(F_1 \text{ min}, F_2 \text{ min}, F_3 \text{ min})$ to the edge $(F_1 \text{ max}, F_2 \text{ max}, F_3 \text{ max})$. We will term these peaks *diagonal peaks*.

The second class of peaks has two identical frequency coordinates and is located on one of three planes which intersect the cube along the face diagonals (Fig. 2). The peaks with identical F_1 and F_2 coordinates arise from the transfer $A \rightarrow A \rightarrow B$. They are caused by a single coherence transfer which occurs in the second mixing period, and hence we call them *single-transfer peaks*. They may be also called *second-transfer peaks* or—indicating the kind of mixing process—*NOESY single-transfer peaks*. Similarly, the peaks with identical F_2 and F_3 coordinates which arise from the process $A \rightarrow B \rightarrow B$ are called *single-transfer peaks* or *first-transfer peaks*. The signals with identical F_1 and F_3 coordinates occur because of a double coherence transfer: $A \rightarrow B \rightarrow A$. They are expected to be much weaker, although still detectable, than the other two kinds of peaks. They will be called *back-transfer peaks*. All three planes intersect at the diagonal of the spectrum.

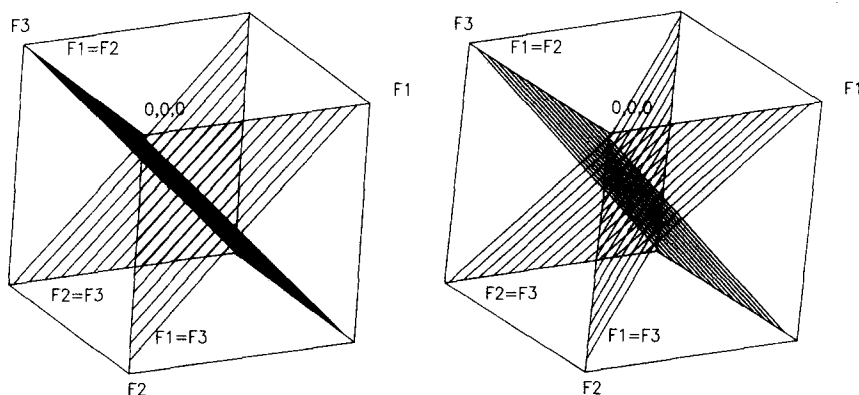


FIG. 2. Positions of the different kinds of peaks in a 3D spectrum. The *single-transfer peaks* which correspond to the cross peaks in 2D spectra occur on the planes with $F_1 = F_2$ and $F_2 = F_3$ coordinates. The former arise from a coherence transfer in the first step, and the latter from a coherence transfer in the second step. Peaks located on the plane with $F_1 = F_3$ coordinates arise from a double coherence transfer with the coherence transferred back to the same spin from which it originated. These peaks are called *back-transfer peaks*. The three planes intersect at the diagonal of the spectrum where the *diagonal peaks* are located. *3D cross peaks* occur anywhere in the spectral volume.

The signals with three different frequency coordinates arising from the transfer $A \rightarrow B \rightarrow C$ will be located anywhere in the cube. These peaks will be called *3D cross peaks*, to ensure that no confusion arises in a parallel discussion of 2D and 3D spectra.

In the above discussion, we have not discussed signals which may occur on a plane of the cube, as they can be removed by phase cycling. They correspond to axial peaks in 2D spectroscopy and will be called *facial peaks*.

THREE-DIMENSIONAL HARTMANN-HAHN-NUCLEAR OVERHAUSER SPECTROSCOPY

The pulse sequences which we have used to record the 3D HOHAHA-NOESY spectra with a reduced spectral width in one or two dimensions are depicted in Fig. 3. The first two sequences (Figs. 3a and 3b) were used to record a spectrum with a reduced spectral widths in F_1 only while the last one (Fig. 3c) results in a 3D spectrum with reduced spectral width in both F_1 and F_2 . The minimum phase cycle is 8 for the first sequence (Fig. 3a), 16 for the second (Fig. 3b), and 32 for the third (Fig. 3c). In all three sequences, water suppression is achieved by means of a jump-return read pulse at the end of the mixing period of the NOESY sequence.

Neglecting the effects of transverse relaxation, the intensity of the 3D cross peaks and back-transfer peaks is given by the product of the efficiency of the two mixing processes. The amplitude of a HOHAHA single-transfer peak is a product of the corresponding cross peaks in a 2D HOHAHA spectrum and the diagonal peaks in the 2D NOESY spectrum, and vice versa for a NOESY single-transfer peak. As there is only a fraction of the equilibrium magnetization transferred into the cross peaks in each of the coherence-transfer steps, the intensity of a 3D cross peak is generally much smaller than that of a single-transfer peak, whose amplitude corresponds to the amplitude of a 2D cross peak.

In the case of 3D HOHAHA-NOESY spectra of proteins, three points must be taken into account with respect to the mixing period of the HOHAHA moiety of the sequence. (i) To facilitate the interpretation of the spectra, the cross peaks should have pure phase absorption lineshapes and, therefore, antiphase terms should be suppressed as much as possible. (ii) The transfer should be as effective as possible. For proteins, this is not entirely trivial as the strong ROE occurring during the mixing process is of opposite sign to the HOHAHA transfer. In this respect the Clean HOHAHA (or Clean TOCSY) approach (23) can be used to compensate the ROE with the NOE as the two effects are of opposite signs. (iii) The frequencies of the transverse components after the spin lock are distributed over the whole spectrum. Consequently, these must be removed using, for example, a semiselective z filter for frequency selection in F_2 (4).

We found that a completely satisfactory solution taking care of these three points is difficult to achieve in 3D spectroscopy. For example, antiphase components can be removed to a large extent in 2D NMR by z filtering (24). This, however, is often not applicable in 3D NMR, as it would increase the measurement time substantially due to the longer phase cycle required. Additional delays in the HOHAHA mixing sequence (e.g., MLEV-17) may lead to a pulse sequence which is too long to be stored in the memory of the pulse programmer of some commercial instruments. For the same reason, it is often not possible to apply a satisfactory phase cycling of all critical phases. The sequence for the spin lock which we used was the MLEV-17 sequence

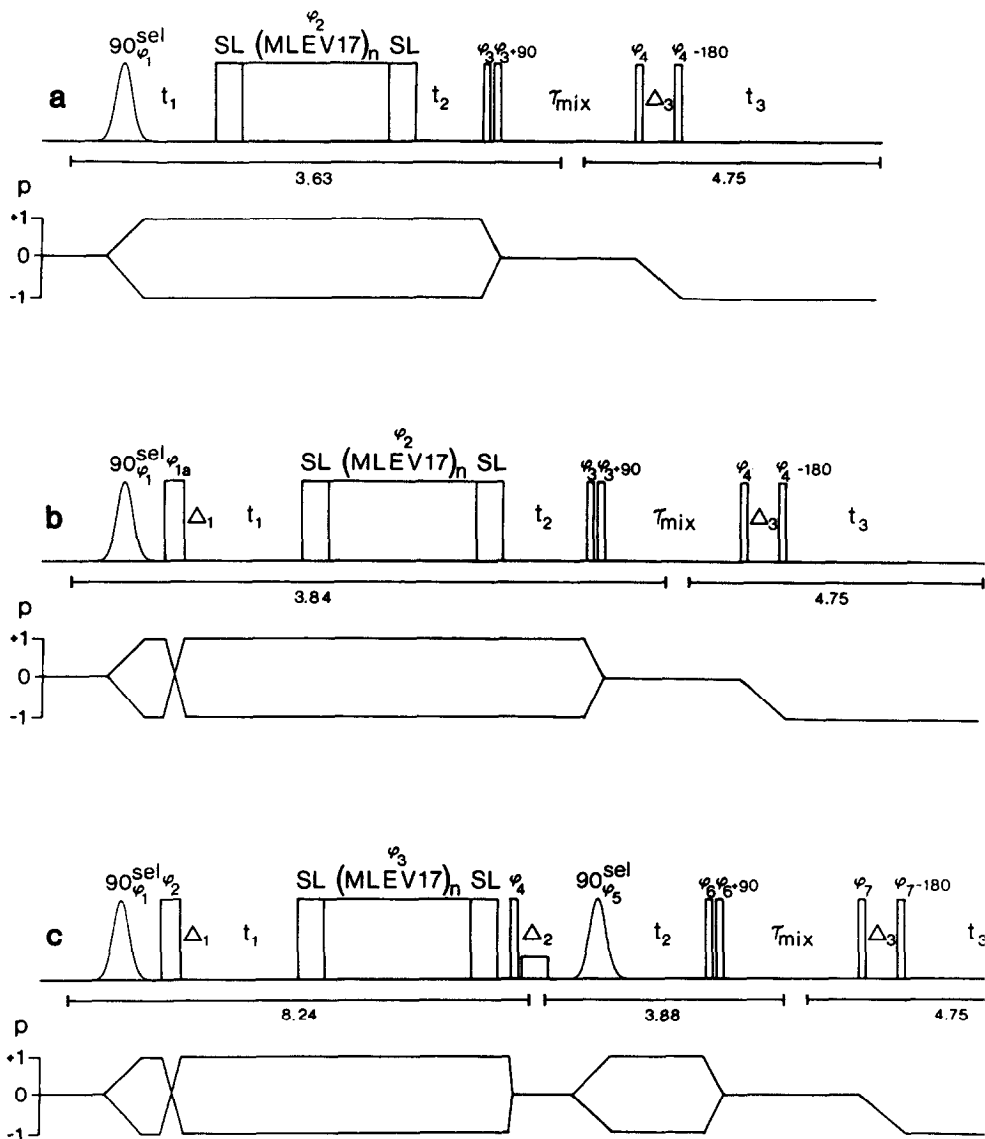


FIG. 3. Pulse sequences used for recording subvolumes of the 3D HOHAHA-NOESY spectrum. St rectangles are pulses with a flip angle of 90° ; wider rectangles are π pulses. Pulse sequences (a) and (b) used to record subvolumes with a reduced spectral width in F_1 only. The difference between the two sequences lies in whether the magnetization is refocused (b) or not (a) after the semiselective pulse. The basic phase cycle for both sequences is the same: $\phi_1 = x, -x, -x, x$; $\phi_2 = 2(x), 2(-x)$; $\phi_3 = x = 4(x), 4(-x)$; receiver = $x, -x, -x, x, -x, x, x, -x$. The phase of the π pulse in sequence (b) alternated to avoid artifacts in the spectrum: $\phi_{1a} = 2(y, -y, -y, y), 2(-y, y, y, -y)$. The spectra recorded with sequence (b) was obtained using mild preirradiation of the water resonance. To minimize artifacts, the phase of the decoupler frequency was inverted after each 16-step phase cycle. The position of the transmitter frequency for the spectra is given below the sequence. The pulse sequence in (c) is used to record a subvolume of the 3D HOHAHA-NOESY spectrum in H_2O with reduced frequency axes both F_1 and F_2 . The first unit—a semiselective HOHAHA experiment—is followed by a semiselective filter which prepares the desired coherences for the NOESY unit. To refocus the chemical-shift preces-

with two long pulses ($\sim 1-2$ ms) at the beginning and the end of the MLEV-17 sequence to destroy antiphase terms (25). In one case, delays within some of the composite pulses (totaling half the HOHAHA mixing time) were added to reduce the ROE by a compensating NOE of equal and opposite sign. To test the quality of the spin lock, a phase-sensitive 2D spectrum was recorded. This showed that the phase anomalies of all diagonal and cross peaks were negligible. The same phase behavior of the signals in F_2 is therefore expected for the 3D spectrum, assuming that zero-quantum coherences generated during the spin-lock period are filtered out by phase cycling as changes of $\Delta p = \pm 1$ are blocked to remove axial peaks. Coherences corresponding to combination lines are filtered out by the NOESY unit which is equivalent to a z filter (26).

Only a few problems arise concerning the NOESY mixing unit of the sequences. First, a very limited phase cycling to block coherences precessing during the mixing time can be used for reasons described above. Second, all approaches described for the suppression of zero-quantum coherences (27) are not applicable. For mixing times longer than 100 ms, however, multiple-quantum coherences do not pose severe problems in protein spectra.

There are several problems associated with the use of semiselective pulses. (i) The amplitudes of the signals in the 3D spectrum are influenced by the excitation profile of the shaped pulses used for semiselective excitation. At the resonance of proton A, the excitation by the pulse is proportional to $\frac{1}{2} \sin \beta_A$, where β_A corresponds to the flip angle of the shaped pulse at this resonance. For the sequence in Fig. 3c, the effect of two pulses must be taken into account. This can be expressed as the product $\frac{1}{2} \sin \beta_A \cdot \frac{1}{2} \sin \beta_B$. If a 3D cross peak involves two protons which are not fully excited, it may be severely attenuated. (ii) The use of soft pulses can introduce severe baseline distortions into the spectrum. These occur because the magnetization precesses during the pulse. To remove such baseline distortions, a π pulse together with a refocusing period can be used after the semiselective pulse. This solution, however, generates another problem: namely, a substantial amount of antiphase magnetization develops during the Gaussian pulse and the refocusing period so that the peaks will no longer be absorptive, especially when small spectral ranges are selected.

We have used sequences with (Fig. 3a) and without (Fig. 3b) refocusing to record 3D spectra with a reduced spectral width in F_1 only. The justification for recording a 3D spectrum without refocusing is that the baseline distortions may be correctable with a polynomial providing the semiselective pulse is short relative to the reciprocal of the spectral width. This approach, however, is only applicable if there are very few large signals (diagonal signals) in the spectral regions of interest. If there are several large signals, the version of the sequence with refocusing (Fig. 3b) must be used to

during the first soft pulse (Gaussian-shaped), a π pulse is applied before t_1 together with a suitable delay. This approach could not be used after the second soft pulse because the necessary additional phase cycling would require too many scans per increment. The length of the delay Δ_1 is approximately half the length of the Gaussian pulse. At 500 MHz, the length of the delay Δ_2 is typically 80 μ s. The position of the transmitter in our experiment is given in ppm below the sequence. The phases are cycled as follows: $\phi_1 = 2(x), 2(-x)$; $\phi_2 = 2(x, -x)$; $\phi_3 = 2(y, y, -y, -y), 2(-y, -y, y, y)$; $\phi_4 = 4(x), 4(-x)$; $\phi_5 = x$; $\phi_6 = 16(x), 16(-x)$; receiver = $4(x), 8(-x), 4(x), 4(-x), 8(x), 4(-x)$.

avoid artifacts. The baseline will then be undistorted, but the phase cycling must be increased by a factor of 2 to avoid artifacts arising from the π pulse, which may lead to a substantial increase in measurement time. By the appropriate adjustment of the acquisition parameters it is possible to obtain useful spectra with both sequences as shown below.

When the spectral region excited with the first pulse contains the C^oH protons special care must be taken of the intense water resonance for both sequences with frequency selection in F_1 . In this case, the water signal is fully excited and cross peaks arising from NH₂ protons exchanging rapidly with the water will become very large due to the substantial equilibrium magnetization of the water. To minimize these cross peaks, the water resonance was mildly presaturated in the spectrum recorded with the pulse sequence in Fig. 3b. The jump–return pulse at the end of the sequence was kept to avoid the necessity of irradiation during the mixing period.

COMPUTATION OF 3D SPECTRA

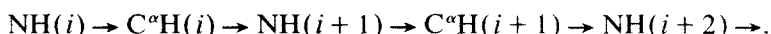
The strategy we have used to process 3D spectra is based on the rationale that it is not necessary to compute the three-dimensional spectrum as a whole (i.e., to handle it in a single data file). It is always possible to process subvolumes of the full three-dimensional spectrum which are of acceptable size. Further, the phase corrections necessary in two of the three dimensions, for example, F_1 and F_3 , may be obtained from the first or—if not possible—from another (F_1, t_2, F_3) spectrum which can be calculated *before* starting the full 3D processing. In these circumstances, it is possible to delete the imaginary parts in these two dimensions immediately after Fourier transformation to save memory space. Even the parameters for the phase correction in F_2 may be found before Fourier transformation of the whole spectrum along t_2 . For example, three or four individual vectors along t_2 may be read out of the three-dimensional data matrix (F_1, t_2, F_3) and transformed. If these vectors contain peaks distributed over the entire spectral width, the appropriate phase correction for F_2 can easily be determined. As a result, the data matrix of the calculated region of the spectrum consists only of the triple real part, which is left after deleting the various imaginary/real combinations. The size of a 3D FID file will not usually be larger than 67 megawords for the experimental setup discussed above, and the spectrum itself can be calculated in manageable portions of 16 megawords. Further details are given under Experimental.

EVALUATION OF THE SPECTRA

The evaluation of 2D NMR spectra is normally carried out in a graphical manner by drawing lines connecting cross peaks on contour plots to indicate connectivities. The connection of two cross peaks by a line parallel to one of the two frequency axes in a protein 2D spectrum indicates that one of the two frequency coordinates of two cross peaks is the same (they are related to the same spin). Hence the other two resonances indicated by the other two frequency coordinates belong either to the same amino acid or to two spatially adjacent amino acids. Correlation experiments yield only the former connectivities, while NOESY spectroscopy yields both intra- and interresidue connections.

In 3D NMR spectroscopy, the connectivity information is either given directly by the three different frequency coordinates of a 3D cross peak or located on perpendicular planes. It is also possible to connect the 3D cross peaks by lines, but not in a simple manner as in 2D spectroscopy. This is illustrated in the following paragraph with an example, for which the HOHAHA-NOESY technique is especially suited.

The sequential assignment of amino residues in a β strand normally proceeds by the detection of $\text{NH}(i) \rightarrow \text{C}^\alpha\text{H}(i)$ cross peaks in a COSY or HOHAHA spectrum and $\text{C}^\alpha\text{H}(i) \rightarrow \text{NH}(i+1)$ cross peaks in a NOESY spectrum. If these cross peaks are observed for several neighboring amino acids one obtains the linear pattern



In a 3D HOHAHA-NOESY spectrum the connection between amino acid i and $i+1$ is simply given by the 3D cross peak with the frequency coordinates $[\text{NH}(i), \text{C}^\alpha\text{H}(i), \text{NH}(i+1)]$ in (F_1, F_2, F_3) . In general, the assignment using 3D will be more reliable than that using 2D if there are C^αH signals or NH signals with accidentally degenerate chemical shifts. The cross peak indicating the connectivity between the amino acids $i+1$ and $i+2$ has coordinates $[\text{NH}(i+1), \text{C}^\alpha\text{H}(i+1), \text{NH}(i+2)]$ and lies in the F_2, F_3 plane with the F_1 frequency coordinate $[\text{NH}(i+1)]$. Since the first cross peak $[\text{NH}(i), \text{C}^\alpha\text{H}(i), \text{NH}(i+1)]$ is located in the F_1, F_2 plane perpendicular to the latter one, which has the F_3 frequency coordinate $[\text{NH}(i+1)]$, these two planes intersect each other in the F_2 vector with the coordinates $F_1, F_3 = [\text{NH}(i+1), \text{NH}(i+1)]$. Examination of the F_1, F_3 projection of the spectrum yields a simple graphical representation of the assignment. The NH-NH cross peaks must be connected by perpendicular lines which meet each other at the diagonal as indicated in Fig. 4a. In 3D frequency space, the ends of these lines are separated by a F_2 vector which is directed from the chemical shift of the $\text{C}^\alpha\text{H}(i)$ proton to the chemical shift of the $\text{C}^\alpha\text{H}(i+1)$. This is shown in Fig. 4b, where two 3D cross peaks are connected by lines to indicate the assignment.

In practical cases, however, a graphical representation of the assignments in the manner described above without suitable software facilities would be more confusing than helpful. The procedure that we used to assign the spectrum in practice was as follows. First, we plotted the relevant F_1, F_3 planes and located all 3D cross peaks. In parallel, we used a three-dimensional peak-picking algorithm and evaluated the spectrum by inspection of the list. Second, we checked the results by inspecting the F_2, F_3 planes. In this way, all three frequencies of the cross peaks could be properly determined, providing there was no overlap.

PATTERN OF 3D CROSS PEAKS IN HOHAHA-NOESY SPECTRA

2D NMR spectra of proteins have been analyzed in detail (7, 8) and the classical coupling pattern in 2D COSY or HOHAHA spectra for each of the individual amino acids and the "space pattern" in 2D NOESY spectra for the different secondary structure elements in proteins are well known. The identification of these patterns usually constitutes the first step in the structural analysis of a protein.

In this section, we show that there are characteristic patterns in 3D HOHAHA-NOESY spectra. The couplings involved in these patterns are those between the NH,

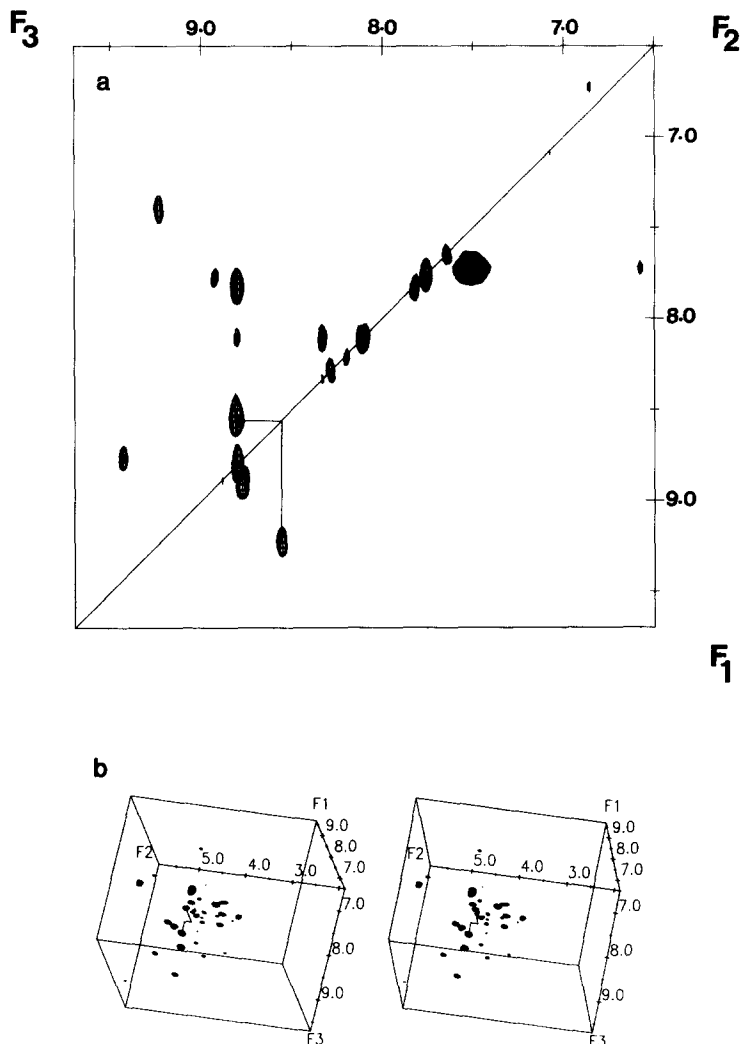


FIG. 4. (a) F_1/F_3 projection of the $\text{NH}(F_1)\text{-C}^\alpha\text{H}/\text{C}^\beta\text{H}(F_2)\text{-NH}(F_3)$ subvolume of the 3D HOHAHA-NOESY spectrum of 6 M α_1 -purothionin in 90% $\text{H}_2\text{O}/10\%$ D_2O recorded with the Fig. 3c sequence. This projection is equivalent to a 2D relayed HOHAHA-NOESY spectrum. Each off-diagonal peak yields sequential information via $\text{NH}(i) \rightarrow \text{NH}(i+1)$ connectivities. This is indicated for the sequence Lys-32-Ile-33-Ser-34. The chemical shifts of the NH protons of these three residues are 9.21, 8.56, and 8.80 ppm, respectively. (b) Stereoview of the same subvolume of the 3D HOHAHA-NOESY spectrum of α_1 -purothionin. The ends of the two lines which were used in (a) to indicate the sequential assignment are connected by a line along F_2 which starts at the chemical shift of the C^αH proton of Lys-32 ($\text{C}^\alpha\text{H}(i)$) and ends at the chemical shift of the C^αH proton of Ile-33 ($\text{C}^\alpha\text{H}(i+1)$). This additional information makes the sequential assignment more reliable because there are two amino acids in α_1 -purothionin whose backbone amide protons resonate at 8.56 ppm.

C^αH , and C^βH protons: ${}^3J_{\text{NH-C}\alpha\text{H}}$, ${}^3J_{\text{C}\alpha\text{H-C}\beta\text{H}(2)}$, ${}^3J_{\text{C}\alpha\text{H-C}\beta\text{H}(3)}$. The values of these coupling constants are indicative of particular conformations of the backbone and side chains. The same three protons are involved in space patterns which are indica-

tive of the different units of secondary structures in a protein. The distances involved in the space patterns are $d_{\alpha N}(i, i+1)$, $d_{NN}(i, i+1)$, $d_{\beta N}(i, i+1)$, $d_{\alpha N}(i, i+2)$, $d_{NN}(i, i+2)$, $d_{\alpha N}(i, i+3)$, $d_{\alpha\beta}(i, i+3)$, $d_{\alpha N}(i, i+4)$ (see Ref. (7) for the notation). There is another space pattern which relates to distances within one amino acid: $d_{N\beta 2}(i, i)$; $d_{N\beta 3}(i, i)$; $d_{\alpha\beta 2}(i, i)$; $d_{\alpha\beta 3}(i, i)$; $d_{N\alpha}(i, i)$. This pattern determines the conformation of the side chains and, if the values of the three-bond coupling between the C $^{\alpha}$ H and the C $^{\beta}$ H protons are known, allows stereospecific assignment of the β protons (28). Additionally, distances between NH and C $^{\beta}$ H protons of different residues far apart in the sequence, as well as long-range NOEs involving side-chain protons, are important in defining the tertiary structure.

In the case of the 3D HOHAHA-NOESY experiment, the expected pattern of the 3D cross peaks will in principle be a cross product of the coupling and space patterns. The amplitudes of the cross peaks will depend *both* on the size of the coupling *and* on the distances. Consequently, many kinds of peaks will be very weak. Nevertheless, certain structural elements show very pronounced characteristics *as* their amplitudes depend on two parameters, rather than on one as in a 2D experiment.

Unfortunately the $^3J_{NH-C\alpha H}$ coupling in α helices is small (~ 4 Hz) and the distances between the adjacent NH protons are not very short (2.8–3 Å), so that only very weak 3D cross peaks of the type $^3J_{NH(i)-C\alpha H(i)}d_{NN}(i, i \pm 1)$ are expected for α -helical elements. All other NOEs characteristic of α helices are even weaker. For a β strand, there is one sequential distance, $d_{\alpha N}$, that can be observed. This distance is very short (~ 2.3 Å) and the vicinal coupling $^3J_{NH-C\alpha H}$ is large, so that very intense 3D cross peaks of the type $J_{NH(i)-C\alpha H(i)}d_{\alpha N(i, i+1)}$ and $J_{NH(i)-C\alpha H(i)}d_{\alpha N(i-1, i)}$ are expected.

For turns, very characteristic patterns are expected, especially in the region of the spectrum where the 3D cross peaks for the transfer C $^{\alpha}$ H(i) \rightarrow NH(i) \rightarrow NH($i \pm 1$) occur. As these cross peaks are expected to be much larger for amino acids located in turns relative to those of amino acids located in an α helix, this region of the 3D HOHAHA-NOESY spectrum can potentially constitute a "fingerprint" of the turns in the protein. For a peptide segment consisting of four amino acids, for example, the cross peaks involving the couplings $^3J_{NH(2)-C\alpha H(2)}$ and $^3J_{NH(3)-C\alpha H(3)}$ are of particular interest. These couplings are involved in six types of cross peaks: $^3J_{NH(2)-C\alpha H(2)}d_{\alpha N}(2, 3)$; $^3J_{NH(2)-C\alpha H(2)}d_{NN}(2, 3)$; $^3J_{NH(3)-C\alpha H(3)}d_{\alpha N}(3, 4)$; $^3J_{NH(2)-C\alpha H(2)}d_{\alpha N}(2, 4)$; $^3J_{NH(3)-C\alpha H(3)}d_{NN}(3, 2)$; $^3J_{NH(3)-C\alpha H(3)}d_{NN}(3, 4)$. Evidence for a type I turn ($\phi_{2,3} = -60^\circ, -90^\circ, \psi_{2,3} = -30^\circ, 0^\circ$; Ref. (29)), for example, can be derived by observing the two cross peaks $^3J_{NH(3)-C\alpha H(3)}d_{NN}(3, 4)$ (9.0 Hz, 2.4 Å) and $^3J_{NH(3)-C\alpha H(3)}d_{NN}(3, 2)$ (9.0 Hz, 2.6 Å), where the first 3D cross peak is expected to be more intense than the second.

3D cross peaks which arise because of an intraresidue NOE between a NH proton and one of the C $^{\beta}$ H protons may be of interest as their amplitudes depend critically on both three-bond couplings and the NOE. Thus it should be possible in principle to obtain stereospecific assignments and an estimate of the side-chain χ_1 torsion angles from the amplitudes of the cross peaks.

EXAMPLE

In this section we present the results of three different 3D acquisitions recorded with the pulse sequences shown in Fig. 3. The two spectra obtained with the se-

quences in Figs. 3a and 3b differ with respect to spectral resolution. The spectrum recorded with the pulse sequence in Fig. 3a was recorded with a very coarse limiting resolution in F_1 and F_2 (0.07 and 0.11 ppm), while that of the other spectrum was much better (0.05 and 0.07 ppm). The first spectrum was used as a test case to assess the extent to which it is possible to interpret a spectrum obtained with such low resolution. The second spectrum was used to focus on a region that was difficult to interpret in the first spectrum due to the poor resolution.

In analyzing the spectra the influence of poor resolution was carefully taken into account. In this respect the following points should be considered. As the first coherence transfer occurs *within* the spin system of an amino acid, the requirement for the assignment of the 3D cross peak is that the cross peak for this transfer in the 2D HOHAHA spectrum is separated sufficiently from other cross peaks. If there are two signals of the *same* residue closer than 0.1 ppm in the spectrum, additional problems arise in the evaluation of the 3D cross peaks from these signals due to the fact that they may occur too close to the single-transfer peaks. An example is cross peaks which arise from the transfer $C^{\beta a}H \rightarrow C^{\beta b}H \rightarrow NH$. If the chemical shifts of the two $C^{\beta}H$ protons are not very different, these cross peaks occur very close to the NOESY single-transfer peaks $C^{\beta a}H \rightarrow C^{\beta b}H \rightarrow NH$ and $C^{\beta b}H \rightarrow C^{\beta a}H \rightarrow NH$, and thus in many cases may not be resolved due to the large size of the NOESY single-transfer peaks relative to the 3D cross peaks.

Both spectra were processed in two parts, one part comprising the full F_1 and F_2 spectral widths and the downfield F_3 region (NH protons), the other comprising the upfield F_3 region with the aliphatic resonances from about 4.5 to 1.0 ppm. As anticipated, it was found that the only useful portion of the 3D spectrum recorded with the Fig. 3a sequence was that comprising the NH region in F_3 . The other part of this 3D spectrum was uninterpretable due to baseline problems. In the spectrum recorded with the refocused sequence (Fig. 3b) both regions could be interpreted.

The 3D spectrum is not symmetric, because, although peaks of the type $C^{\alpha}H(i) \rightarrow C^{\beta}H(i) \rightarrow NH(i)$ and $C^{\alpha}H(i) \rightarrow NH(i) \rightarrow C^{\beta}H(i)$ should both appear, only the first type of peak was actually observed. There are several reasons for this. The majority of couplings between the NH protons and the $C^{\alpha}H$ protons are small in α_1 -purothionin, whereas the coupling from the $C^{\alpha}H$ proton to at least one $C^{\beta}H$ proton is usually large. Further, there is more t_1/t_2 noise in the aliphatic F_3 region of the spectrum.

As a result, the low-field F_3 region is the most interesting in the two spectra. There are only a limited number of single-transfer peaks and a large number of 3D cross peaks. The cross peaks are due to transfers of the type $C^{\alpha}H(i) \rightarrow C^{\beta}H(i) \rightarrow NH(i)$, $C^{\beta a}H(i) \rightarrow C^{\beta b}H(i) \rightarrow NH(i)$, $C^{\alpha}H(i) \rightarrow C^{\beta}H(i) \rightarrow NH(i+1)$, $C^{\beta a}H(i) \rightarrow C^{\beta b}H(i) \rightarrow NH(i+1)$, or $C^{\alpha}H(i) \rightarrow C^{\beta}H(i) \rightarrow NH(x)$ and $C^{\beta a}H(i) \rightarrow C^{\beta b}H(i) \rightarrow NH(x)$. These regions of the spectra are shown in Figs. 5 and 6.

In the upfield F_3 region, which could only be evaluated in the spectrum recorded with the Fig. 3b sequence, trivial back-transfer peaks of the type $C^{\beta a}H(i) \rightarrow C^{\beta b}H(i) \rightarrow C^{\beta a}H(i)$ and $C^{\alpha}H(i) \rightarrow C^{\alpha b}H(i) \rightarrow C^{\alpha b}H(i)$ were predominantly observed apart from the expected diagonal and single-transfer peaks with one exception: there is a cross peak with the frequency coordinates of Cys-16($C^{\alpha}H$)/Cys-16($C^{\beta}H$)/

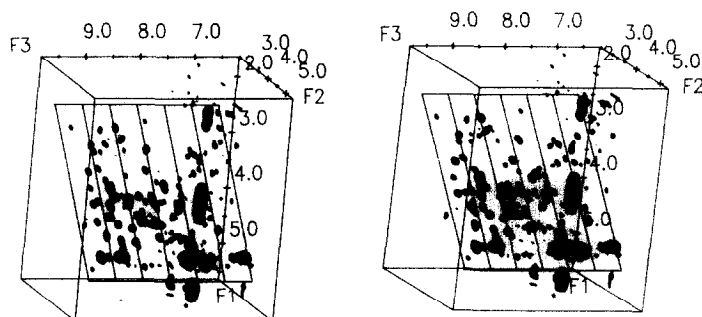


FIG. 5. Stereoview of the subvolume of the 3D HOHAHA-NOESY spectrum comprising the $C^{\alpha}H$ and $C^{\beta}H$ regions in F_1 and F_2 and the NH region in F_3 . This subvolume was recorded with the Fig. 3a pulse sequence. Baseline corrections in all three dimensions were applied. The lines in the spectrum indicate the plane, on which the NOESY single-transfer peaks are located. There is a large signal with coordinates 4.75/4.75/7.48 ppm in $F_1/F_2/F_3$, which is a NOESY single-transfer peak arising from chemical exchange between water and Lys NH $_3$ protons. Because of the broadness of this peak, large baseline distortions are still left in the F_1 and F_3 sections through this signal after baseline correction. Therefore, only positive signals are shown in the figure. All other 3D cross peaks and single-transfer peaks have only minor negative components. The contour level shown is drawn at four times the highest noise level. A further impression of the amplitudes of the peaks can be obtained from Fig. 9.

Gly-27($C^{\alpha\beta}H$) which permitted the assignment of a strong NOE that was not possible to assign previously from the 2D NMR spectra (12).

The 3D cross peaks found in the regions with the low-field F_3 frequency (i.e., NH protons) in the two spectra recorded with the Figs. 3a and b pulse sequences are listed in Table 1. No single-transfer peaks and back-transfer peaks are listed.

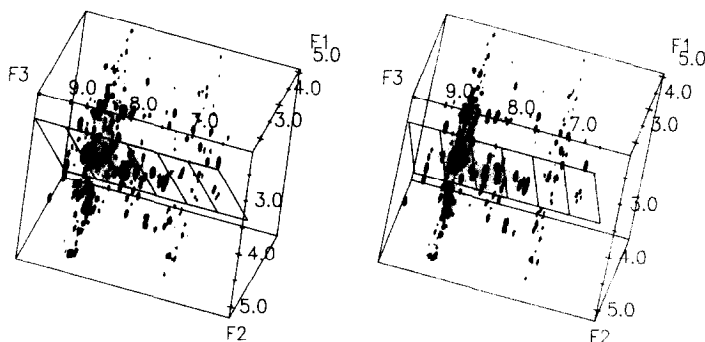


FIG. 6. Stereoview of the same subvolume of the 3D HOHAHA-NOESY spectrum as shown in Fig. 5 but obtained with the Fig. 3b pulse sequence and mild preirradiation of the water resonance. For this reason and because the semiselective pulse at the beginning of the sequence does not excite the water substantially, the large signal in the spectrum shown in Fig. 5 has disappeared. The lines indicate the plane on which the NOESY single-transfer peaks are located. Due to the refocusing pulse, only weak baseline distortions in F_1 are observed. The two planes with t_1/t_2 noise are due to experimental artifacts. There is only one 3D cross peak which shows antiphase structure in F_2 and F_3 (Ser-38 $C^{\alpha\beta}H \rightarrow C^{\alpha}H \rightarrow NH$, below the plane). The two $C^{\beta}H$ protons of this residue are strongly coupled.

TABLE 1
3D Cross Peaks Observed in the 3D HOHAHA-NOESY Spectra of α_1 -Purothionin Recorded with the Fig. 3a and b Pulse Sequences

Residue	$\delta(\text{C}^\circ\text{H})$	Intraresidue	Interresidue
Lys-1			
Ser-2	4.66		$\beta_a\beta_b,\text{NH}(3)$; $\beta_a\alpha,\text{NH}(3)$
Cys-3	8.76	$\beta_b\beta_a,\text{NH}$	$\beta_a\alpha,\text{NH}(4)$; $\beta_b\alpha,\text{NH}(4)$
Cys-4	5.21	$\beta_b\beta_a,\text{NH}$	$\beta_a\alpha,\text{NH}(5)$; $\beta_b\alpha,\text{NH}(5)$
Arg-5	4.24	$\alpha\beta_b,\text{NH}$; $\delta_{a,b}\beta_b,\text{NH}$	
Ser-6	4.77		$[\alpha\text{NH},\text{NH}(7)]$; $[\beta_b\beta_a,\text{NH}(7)]$ $\beta_a\beta_b,\text{NH}(7)$; $\beta_a\beta_b,\text{NH}(8)$
Thr-7	3.90	$\alpha\beta,\text{NH}$; $\beta\alpha,\text{NH}$	$\alpha\beta,\text{NH}(8)$
Leu-8	4.09	$\alpha\beta_{a,b},\text{NH}$; $\alpha\beta_b,\text{NH}$	$\alpha\beta_a,\text{NH}(9)$
Gly-9	4.44, 3.89	$\alpha_a\alpha_b,\text{NH}$; $\alpha_b\alpha_a,\text{NH}$	
Arg-10	4.31		
Asn-11	4.48	$\alpha\beta_{a,b},\text{NH}$; $\beta_a\beta_b,\text{NH}$; $\beta_{a,b}\alpha,\text{NH}$	
Cys-12	4.07	$\beta_b\beta_a,\text{NH}$	$\alpha\beta,\text{NH}(13)$
Tyr-13	3.58	$\alpha\beta_b,\text{NH}$; $\beta_b\beta_a,\text{NH}$; $\beta_b\alpha,\text{NH}$ $\beta_b\beta_a,\epsilon\text{H}$; $\alpha\beta_{a,b}\epsilon\text{H}$	$\alpha\beta_{a,b},\text{NH}(14)$
Asn-14	4.22	$\alpha\beta_b,\text{NH}$; $\beta_b\alpha,\text{NH}$; $\alpha\beta_b,\text{NH}_2$	
Leu-15	4.13	$\alpha\beta_{a,b},\text{NH}$; $\alpha\beta_b,\text{NH}$	
Cys-16	4.07	$\alpha\beta_b,\text{NH}$; $\alpha\beta_a,\text{NH}$ $\beta_b\alpha,\text{NH}$	$\alpha\beta_a,\text{NH}(17)$
Arg-17	4.13		
Ala-18	4.14	$\alpha\beta,\text{NH}$	
Arg-19	4.58		$\alpha\text{NH},\text{NH}(20)$
Gly-20	4.43, 3.46	$\alpha_a\alpha_b,\text{NH}$; $\alpha_b\alpha_a,\text{NH}$	$\alpha_1\alpha_2,\text{NH}(21)$; $\alpha_a\alpha_b,\text{NH}(21)$
Ala-21	4.25	$\alpha\beta,\text{NH}$	$\alpha\beta,\text{NH}(22)$
Gln-22	3.82	$\alpha\beta_{a,b},\text{NH}$	
Lys-23	3.87	$\alpha\beta_{a,b},\text{NH}$	
Leu-24	4.13	$\alpha\beta_{a,b},\text{NH}$	$\alpha\beta_{a,b},\text{NH}(25)$
Cys-25	4.48	$\alpha\beta_b,\text{NH}$	
Ala-26	3.91	$\alpha\beta,\text{NH}$	$\alpha\beta,\text{NH}(26)$
Gly-27	4.05, 3.93	$\alpha_a\alpha_b,\text{NH}$; $\alpha_b\alpha_a,\text{NH}$	
Val-28	3.89	$\alpha\gamma,\text{NH}$; $\alpha\beta,\text{NH}$	
Cys-29	4.82	$\beta_b\beta_a,\text{NH}$; $\alpha\beta_{a,b},\text{NH}$	
Arg-30	4.12		
Cys-31	5.40		
Lys-32	4.31		
Ile-33	4.46		
Ser-34	4.61		
Ser-35	4.48		
Gly-36	4.19, 3.83	$\alpha_a\alpha_b,\text{NH}$; $\alpha_b\alpha_a,\text{NH}$	$\alpha_a\alpha_b,\text{NH}(37)$; $\alpha_b\alpha_a,\text{NH}(37)$
Leu-37	4.20		

TABLE 1—Continued

Residue	$\delta(C^\alpha H)$	Intraresidue	Interresidue
Ser-38	4.65	<u>$\beta_{a,b}\alpha,NH$</u>	$\alpha\beta_{a,b},NH(39)$; $\beta_{a,b}\alpha,NH(39)$
Cys-39	4.97	<u>$\beta_b\beta_a,NH$</u>	
Pro-40	4.50		$\beta_b\alpha,NH(41)$; [$\beta_a\alpha,NH(41)$]
Lys-41	3.95		
Gly-42	4.03, 3.61		
Phe-43	4.53		
Pro-44	4.64		
Lys-45	4.31		

Note. Italic letters indicate peaks which occur only in the spectrum recorded with the Fig. 3b pulse sequence, or which could only be interpreted in this spectrum due to the better resolution. Underlined peaks occurred in both spectra. Only resolved 3D cross peaks are listed. Single-transfer peaks, back-transfer peaks, and diagonal peaks are not listed. 3D cross peaks in brackets are weak. The $C^\beta H$ protons and $C^\alpha H$ protons of Gly labeled with a subscript "a" occur at higher δ .

The peaks observed in the spectrum recorded with the Fig. 3c sequence using frequency selection in both F_1 and F_2 are listed in Table 2. The $NH(F_1)/C^\alpha H(F_2)/NH(F_3)$ portion of the spectrum is shown in Fig. 4. In this subvolume of the 3D

TABLE 2
3D Cross Peaks in the 3D HOHAHA-NOESY Spectrum Recorded Using the
Fig. 3c Pulse Sequence with Frequency Selection in F_1 and F_2

(A) $NH(i) \rightarrow C^\alpha H(i) \rightarrow NH(i+1)$	(B) $NH(i) \rightarrow C^\alpha H(i) \rightarrow \text{aliphatic}(x)$
Ser-2, Cys-3	Ser-2, Ser-2 β_b
Cys-3, Cys-4	
Ser-6, Thr-7	Ser-6, Lys-45 β_a/γ
	Ala-18, Ala-18 β
	Arg-19, Arg-19 β_b
	Arg-19, Arg-19 $\gamma_{a,b}$
Ala-21, Gln-22	Ala-21, Ala-21 β
Arg-30, Cys-31	Arg-30, Arg-30 β_a or Gln-22 $\beta_{a,b}$
Lys-32, Ile-33	
Ile-33, Ser-34	Ile-33, Ile-33 $\delta/\gamma Me$
Gly-36, Leu-37	Gly-36, Gly-36 $\alpha_{a,b}$
	Leu-37, Leu-37 $\beta_{a,b}$ Leu-37,
	Leu-37 $\delta Me_{a,b}$
Ser-38, Cys-39	Ser-38, Ser-38 $\beta_{a,b}$
	Gly-42, Gly-42 $\alpha_{a,b}$
	Lys-45, Lys-45 β_b ; Lys-45, Lys-45 γ/β_a

Note. (A) Peaks in the subvolume of the low-field region of F_3 comprising all 3D cross peaks involving the transfer $NH(i) \rightarrow C^\alpha H(i) \rightarrow NH(i+1)$. (B) Peaks in the subvolume of the upfield region of F_3 comprising all transfers involving the $NH \rightarrow C^\alpha H$ connectivity mediated by scalar coupling in the first step.

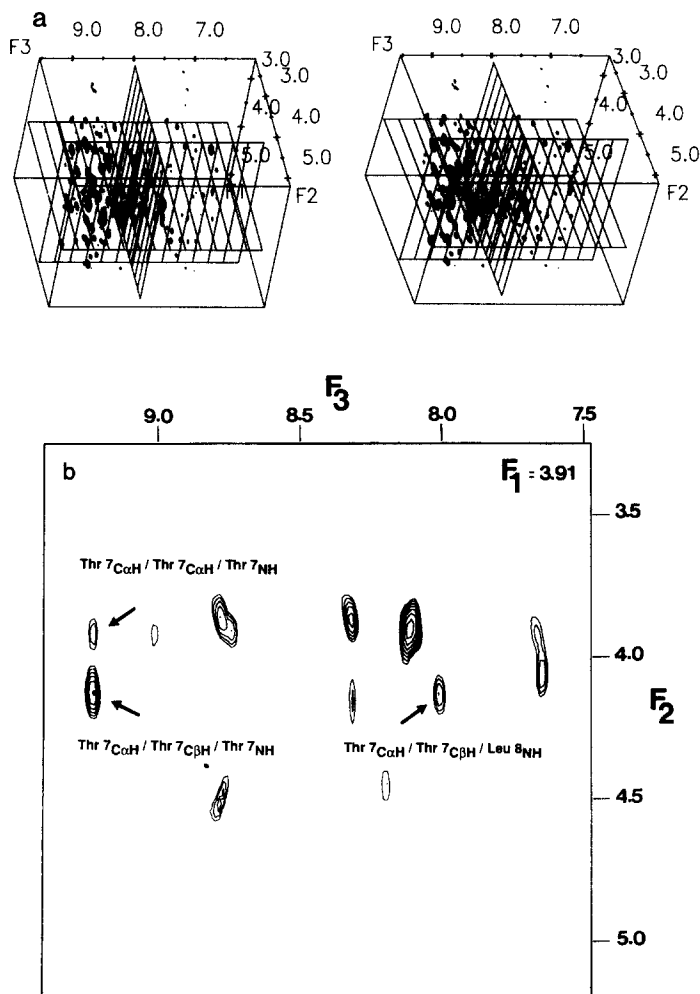
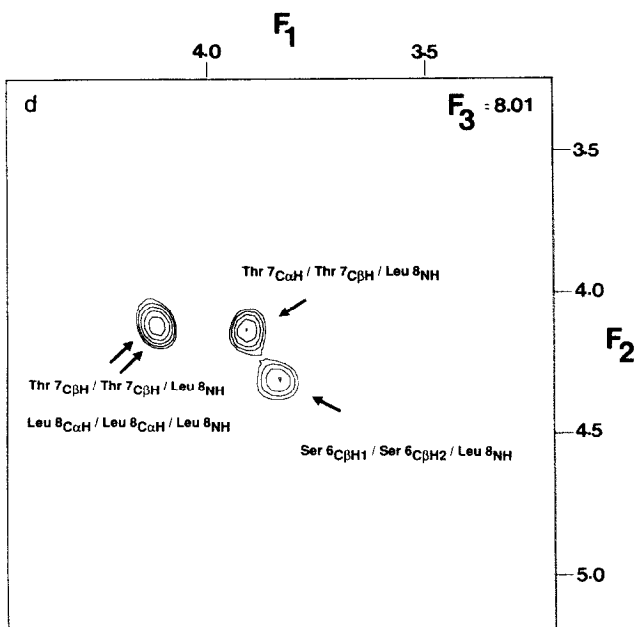
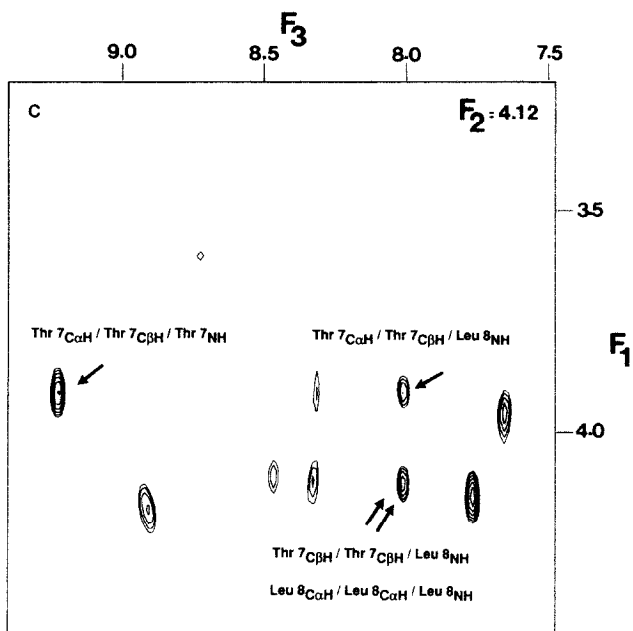
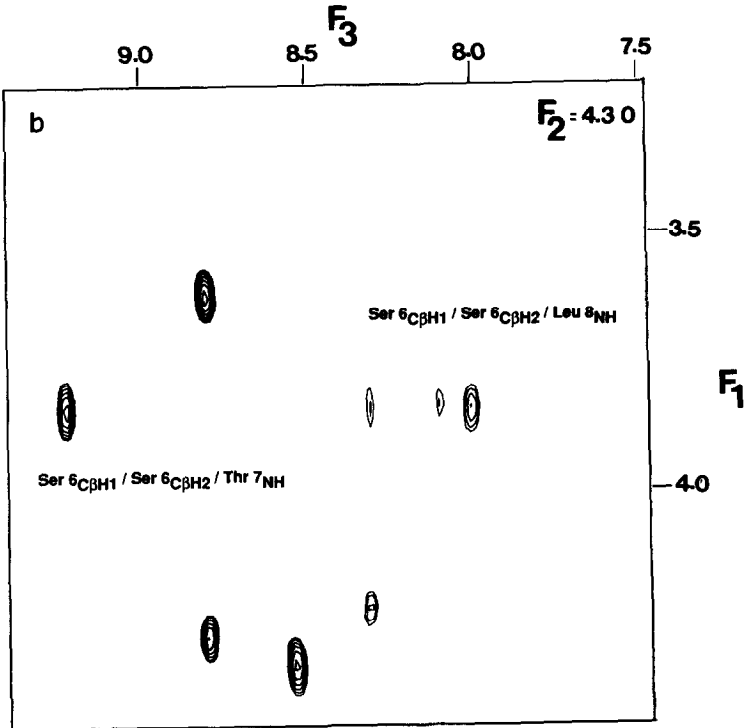
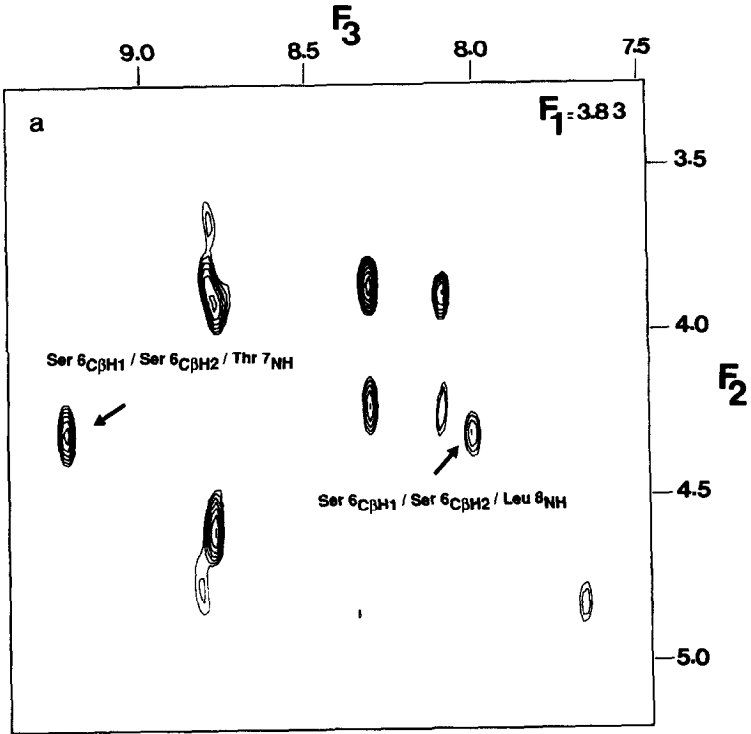


FIG. 7. (a) The same spectrum as that in Fig. 6, but with the cross planes indicated. (b) Cross plane taken at $F_1 = 3.91$ ppm. There are two interesting 3D cross peaks. One with the frequency coordinates $3.91/4.12/9.23$ ppm in $F_1/F_2/F_3$ which arises from the transfer Thr-7($C^\alpha H$) \rightarrow Thr-7($C^\beta H$) \rightarrow Thr-7(NH); the other with the chemical shifts $3.91/4.12/8.01$ ppm arising from the transfer Thr-7($C^\alpha H$) \rightarrow Thr-7($C^\beta H$) \rightarrow Leu-8(NH). In the same cross plane, there is a weak NOESY single-transfer peak with the frequency coordinates $3.91/3.91/9.23$ ppm. The comparison of the amplitude of this cross peak with the amplitudes of the 3D cross peak at $3.91/4.12/9.23$ ppm allows the qualitative conclusion that the $C^\beta H$ proton of Thr-7 is much closer to its own NH proton than to its own $C^\alpha H$ proton. Further, the distance from the $C^\beta H$ proton of Thr-7 to its own NH proton is much shorter than that to Leu-8 NH proton. This can be concluded from a comparison of the amplitudes of the two 3D cross peaks, because they both arise from the same HOHAHA transfer. None of these results is trivial because the $C^\alpha H$ proton of Leu-8 and the $C^\beta H$ proton of Thr-7 have almost identical chemical shifts (~ 4.09 ppm; Ref. (12)). In the 2D NOESY spectrum, there is a cross peak at $F_1 = 4.10$ ppm/ $F_2 = 8.01$ ppm, which could be a cross peak between the $C^\alpha H$ proton of Leu-8 and its own NH proton or between the $C^\beta H$ proton of Thr-7 and the NH proton of Leu-8 (12). (c) The corresponding peak is shown in the cross plane taken at $F_2 = 4.12$ ppm and it has the frequency coordinates $4.12/4.11/8.01$ ppm. The amplitude of the cross peak with the same F_3 chemical shift suggests that the NOESY single-transfer peak consists mainly of the NOE between Thr-7($C^\beta H$) and Leu-8($C^\alpha H$). (d) An impression of the resolution of the spectrum can be obtained from the cross plane taken at $F_3 = 8.01$ ppm which shows the single-transfer peak mentioned in (c) and two 3D cross peaks, one arising from the transfer Thr-7($C^\alpha H$) \rightarrow Thr-7($C^\beta H$) \rightarrow Leu-8(NH), and the other by the transfer



Ser-6($C^{\beta a}H$) \rightarrow Ser-6($C^{\beta b}H$) \rightarrow Leu-8(NH). The chemical shift of the Thr protons is 3.91 and 4.10 ppm, and the chemical shift of the two Ser protons is 3.84 and 4.29 ppm. This cross plane corresponds to a 2D HOHAHA spectrum in which resonances having a NOE to Leu-8(NH) are selectively displayed. Although the peaks are relatively broad, their positions can be determined to the accuracy of the digital resolution due to the reduced overlap in the 3D spectrum.



HOHAHA-NOESY, peaks with the transfer $\text{NH} \rightarrow \text{C}^\alpha\text{H}$ in the first step occur. As can be seen from the data in Table 2, only those residues which have a large coupling show 3D cross peaks of appreciable size. Hence this region contains exclusively peaks involving residues located in turns or β strands.

A few examples illustrating the value of 3D spectroscopy are shown in Figs. 7 to 9. One good example for the determination of different contributions found in one cross peak of the 2D NOESY spectrum by 3D spectroscopy is the NOE between the C^βH proton of Thr-7 and the NH of Leu-8 which was found by means of the 3D cross peak between Thr-7(C^αH), Thr-7(C^βH), and Leu-8(NH) (3.90, 4.09, and 8.01 ppm) (Fig. 7). This is not a trivial finding as the C^αH proton of Leu-8 resonates at exactly the same chemical shift as the C^βH proton of Thr-7, so that the cross peak in the 2D NOESY spectrum also contains an intraresidue NOE. To give an impression of the size of the peak, the corresponding slice of the 3D spectrum is shown in Fig. 7. Figure 8 shows two cross peaks which involve a transfer from Ser-6($\text{C}^{\beta\text{a}}\text{H}$) to Ser-6($\text{C}^{\beta\text{b}}\text{H}$) by a large 3J coupling and from there to the NH proton of Thr-7 and to the NH proton of Leu-8. This confirms nicely the assignment made previously by 2D NOESY spectroscopy (12). An example of cross peaks arising in a turn region is shown in Fig. 9 where a strong cross peak indicates the transfer Arg-19(C^αH) \rightarrow Arg-19(NH) \rightarrow Gly-20(NH). There is a small 3D cross peak to Ala-18(NH) visible in the same slice, which is positioned at $\delta F_3 = 7.22$ ppm, well separated from the band of t_1/t_2 noise at 7.14 ppm. The intensity of this peak can be compared to the intensity of the other 3D cross peak to obtain the relative size of the NOE, because they result from the same HOHAHA transfer. This indicates that the NOE to the NH of Ala-18 is much weaker than that to the NH of Gly-20.

EXPERIMENTAL

All experiments were performed on a Bruker AM 500 spectrometer equipped with a selective excitation unit. Quadrature detection in F_1 and F_2 was achieved using the time proportional incrementation method (30, 31). The data were processed with 3D FT software developed for a Convex C1XP computer as described in the section on computation of 3D spectra. Prior to the Fourier transformation, appropriate Lorentz to Gauss transformations were applied. Baseline corrections with a polynomial of degree 6 or less in all three dimensions were applied after Fourier transformation. In some cases, the baseline correction in F_1 and F_3 was performed before the last FT. The data recorded with the sequences shown in Figs. 3a and 3b were processed with the full spectral width in F_1 and F_2 , and a quarter or less of the spectral width in F_3 . The number of points used was $128 \times 512 \times 256$ for the spectrum in Figs. 6, 7, and 8 and $256 \times 512 \times 186$ for the spectrum in Figs. 5 and 9. The spectra were displayed on a Evans and Sutherland PS390 interactive color graphics system using a slightly modified version (3) of FRODO (32).

FIG. 8. Cross planes taken at (a) $F_1 = 3.83$ ppm and (b) $F_2 = 4.30$ ppm. There are two 3D cross peaks involving the C^βH protons of Ser-6; one arises from a NOE between the C^βH proton with the higher chemical shift and the NH proton of Thr-7, and the other from a NOE between the same C^βH proton and the NH proton of Leu-8. Cross peaks involving a NOE between the other C^βH proton and the two NH protons are not observed.

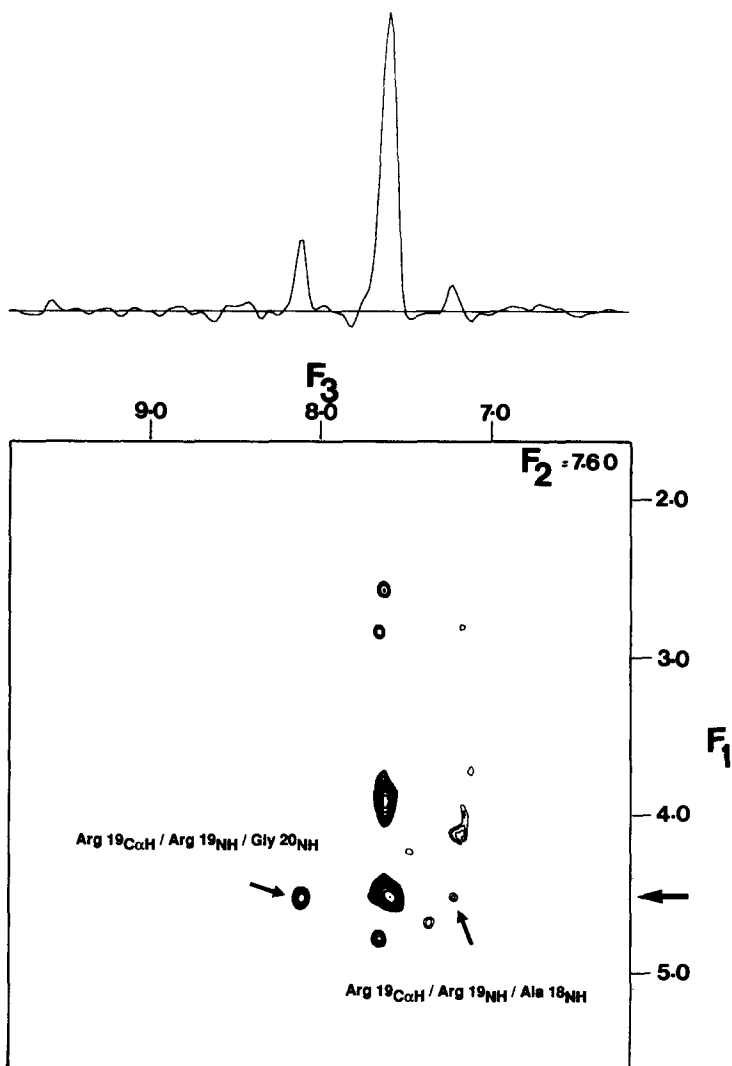


FIG. 9. Cross plane taken at $F_2 = 7.60$ ppm from the spectrum recorded with the Fig. 3a sequence. The two 3D cross peaks indicated arise from the transfers Arg-19($C^{\alpha}H$) \rightarrow Arg-19(NH) \rightarrow Gly-20(NH) and Arg-19($C^{\alpha}H$) \rightarrow Arg-19(NH) \rightarrow Ala-18(NH). The difference in the amplitudes of the two cross peaks indicates the different sizes of the NOEs, because they involve the same HOHAHA transfer. Only positive levels are shown. Very broad, negative levels are observed around the strong single-transfer peaks with the F_3 chemical shift at 7.6/7.7 ppm and along the ridge of t_1/t_2 noise around 7.15 ppm. The lowest level drawn is 31,600, and the highest is 501,000. An impression of the signal-to-noise can be obtained from the cross section shown above the cross plane taken along $F_3 = 4.6$ ppm (see arrow).

The parameters for the spectrum recorded with the Fig. 3a sequence are as follows (order of numbers is $F_1/F_2/F_3$): spectral width, 2000/5882/10,000 Hz; number of collected data points, 64/120/1024; limiting resolution, 0.07/0.11/0.023 ppm; digital resolution was improved by one- or twofold zero-filling; length of the Gaussian

pulse (truncation level was 1%), 2.2 ms; mixing times, 32 ms (HOHAHA) and 200 ms (NOESY); length of one transient, 1.4 s; number of transients per increment, 8.

The parameters for the spectrum recorded with the Fig. 3b sequence are spectral width, 1250/6250/7042 Hz; number of collected data points, 64/200/1024; limiting resolution, 0.05/0.07/0.016 ppm; the digital resolution was again improved by one- or twofold zero-filling; length of the Gaussian pulse (truncation level was 1%), 4 ms; mixing times, 39 ms (HOHAHA) and 220 ms (NOESY); length of one transient, 1.2 s; number of transients per increment, 16.

The parameters for the spectrum recorded with the Fig. 3c sequence can be taken from Ref. (4).

CONCLUSIONS

Three-dimensional high-resolution NMR spectroscopy can yield valuable information for the structural analysis of proteins. As has been shown by the analysis of several portions of the 3D HOHAHA-NOESY spectrum of α_1 -purothionin, 3D NMR techniques are sensitive enough to provide supplementary data to those already obtained by 2D NMR. Characteristic cross-peak patterns for certain types of regular secondary structure elements, such as turns and β strands, can easily be detected in 3D HOHAHA-NOESY spectra.

Subvolumes of a full ^1H NMR 3D spectrum may be recorded by selecting a spectral range either in two dimensions or in the F_1 dimension only, as shown for the example of the 3D HOHAHA-NOESY technique, for which the amount of data collected can be handled without major problems.

ACKNOWLEDGMENTS

This work was supported in part by Grant 321-4003/0318909A from the Bundesministerium für Forschung und Technologie, Grant Gr. 658/4-1 from the Deutsche Forschungsgemeinschaft, and by the Intramural AIDS Targeted Antiviral Program of the Office of the Director of the National Institutes of Health (G.M.C. and A.M.G.). We thank Dr. C. Griesinger for useful discussions.

REFERENCES

1. C. GRIESINGER, O. W. SØRENSEN, AND R. R. ERNST, *J. Magn. Reson.* **73**, 574 (1987).
2. C. GRIESINGER, O. W. SØRENSEN, AND R. R. ERNST, *J. Am. Chem. Soc.* **109**, 7227 (1987).
3. H. OSCHKINAT, C. GRIESINGER, P. J. KRAULIS, O. W. SØRENSEN, R. R. ERNST, A. M. GRONENBORN, AND G. M. CLORE, *Nature (London)* **332**, 374 (1988).
4. H. OSCHKINAT, G. M. CLORE, AND A. M. GRONENBORN, *J. Magn. Reson.* **81**, 212 (1989); G. W. VUISTER, R. BOELENS, AND R. KAPTEIN, *J. Magn. Reson.* **80**, 176 (1988).
5. S. W. FESIK AND E. R. P. ZUIDERWEG, *J. Magn. Reson.* **78**, 588 (1988).
6. D. MARION, L. E. KAY, S. W. SPARKS, D. A. TORCHIA, AND A. BAX, *J. Am. Chem. Soc.*, in press (1988).
7. K. WÜTHRICH, "NMR of Proteins and Nucleic Acids," Wiley, New York, 1986.
8. G. M. CLORE AND A. M. GRONENBORN, *Protein Eng.* **1**, 275 (1987).
9. L. BRAUNSCHWEILER AND R. R. ERNST, *J. Magn. Reson.* **53**, 521 (1983).
10. D. G. DAVIS AND A. BAX, *J. Am. Chem. Soc.* **107**, 2821 (1985).
11. J. JEENER, B. H. MEIER, P. BACHMANN, AND R. R. ERNST, *J. Chem. Phys.* **71**, 4546 (1979).
12. G. M. CLORE, D. K. SUKUMARAN, A. M. GRONENBORN, M. M. TEETER, M. WHITLOW, AND B. L. JONES, *J. Mol. Biol.* **193**, 571 (1987).

13. G. M. CLORE, M. NILGES, D. K. SUKUMARAN, A. T. BRÜNGER, M. KARPLUS, AND A. M. GRONENBORN, *EMBO J.* **5**, 2729 (1986).
14. W. P. AUE, E. BARTHOLDI, AND R. R. ERNST, *J. Chem. Phys.* **64**, 2229 (1976).
15. R. J. SUTHERLAND AND J. M. S. HUTCHINSON, *J. Phys. E* **11**, 79 (1978).
16. C. J. BAUER, R. FREEMAN, T. FRENKIEL, J. KEELER, AND A. J. SHAKA, *J. Magn. Reson.* **58**, 442 (1984).
17. R. BRAUSCHWEILER, J. C. MADSEN, C. GRIESINGER, O. W. SØRENSEN, AND R. R. ERNST, *J. Magn. Reson.* **73**, 380 (1987).
18. J. CAVANAGH, J. P. WALTHO, AND J. KEELER, *J. Magn. Reson.* **74**, 386 (1987).
19. P. PLATEAU AND M. GUERON, *J. Am. Chem. Soc.* **104**, 731 (1982).
20. G. EICH, G. BODENHAUSEN, AND R. R. ERNST, *J. Am. Chem. Soc.* **104**, 3731 (1982).
21. G. WAGNER, *J. Magn. Reson.* **57**, 497 (1984).
22. H. KESSLER, H. OSCHKINAT, C. GRIESINGER, AND W. BERMEL, *J. Magn. Reson.* **70**, 106 (1986).
23. C. GRIESINGER, G. OTTING, K. WÜTHRICH, AND R. R. ERNST, *J. Am. Chem. Soc.* **110**, 7870 (1988).
24. M. RANCE, *J. Magn. Reson.* **74**, 557 (1987).
25. A. BAX AND D. G. DAVIS, *J. Magn. Reson.* **65**, 355 (1985).
26. O. W. SØRENSEN, M. RANCE, AND R. R. ERNST, *J. Magn. Reson.* **56**, 527 (1984).
27. M. RANCE, G. BODENHAUSEN, G. WAGNER, K. WÜTHRICH, AND R. R. ERNST, *J. Magn. Reson.* **62**, 497 (1985).
28. G. WAGNER, W. BRAUN, T. F. HAVEL, T. SCHAUMANN, N. GO, AND K. WÜTHRICH, *J. Mol. Biol.* **196**, 611 (1987).
29. J. S. RICHARDSON, in "Advances in Protein Chemistry" (C. B. Anfinsen, J. T. Edsall, and F. M. Richards, Eds.), Vol. 34, p. 167, Academic Press, New York, 1981.
30. A. G. REDFIELD AND S. D. KUNTZ, *J. Magn. Reson.* **19**, 250 (1975).
31. R. R. ERNST, G. BODENHAUSEN, AND A. WOKAUN, "Principles of Nuclear Magnetic Resonance in One and Two Dimensions," Clarendon, Oxford (1986).
32. T. A. JONES, *J. Appl. Crystallogr.* **11**, 268 (1978).